

## Research Article

## Open Access

Chen CY, Li GY, Zhang L, Huang XH, Cheng D, Wu SC, Xu CZ, Zhou JH\*, Xun L\*

# MicroRNA delivery mediated by PEGylated polyethylenimine for prostate cancer therapy

<https://doi.org/10.1515/chem-2018-0138>

received January 24, 2018; accepted April 10, 2018.

**Abstract:** A microRNA (miRNA) nanomedicine PEG-PEI/miR-221/222 was synthesized based on PEGylated polyethylenimine PEG-PEI and used to transfect prostate cancer cells (PC-3) *in vitro*. Gel retardation assay confirmed the formation of nanomedicine, of which the zeta potential and particle size were determined by dynamic light scattering. Its cytotoxicity was analyzed by CCK-8 assay while its transfection efficiency was analyzed by flow cytometry. Cell uptake and intracellular distribution of nanoparticles were evaluated using laser confocal microscopy. RT-PCR and western-blot assays were conducted to verify the regulation of SIRT1 target gene. We found that the properties of the nanocomplexes of miRNA and PEG-PEI depended on N/P ratios. At higher N/P ratio, accompanied by higher zeta potential and higher cytotoxicity, PEG-PEI is needed to completely condense the miRNA into small particles with uniform size distribution. Under an N/P ratio of 20, high transfection efficiency and low carrier cytotoxicity were obtained simultaneously in PC-3 cells *in vitro*. Consequently, the SIRT1 expression was up-regulated due to the nanoparticle-delivered miR-221/222, which resulted in effective inhibition of PC-3 cells. Our study revealed the PEG-PEI/miR-221/222 nanomedicine as a prospective alternative for treatment of advanced prostate cancer and also lays a foundation for future *in vivo* investigation.

**Keywords:** non-viral vector; prostate cancer; microRNA delivery; nanomedicine; SIRT1 gene.

## Abbreviations

PCa, Prostate cancer; RNAi, RNA interference; PEI, polyethyleneimine; PEG, polyethylene glycol; CCK-8, Cell Counting Kit; EB, ethidium bromide; DEPC, Diethyl pyrocarbonate; Cy3, cyanine 3; DAPI, 4',6-diamidino-2-phenylindole; EDTA, ethylenediaminetetraacetic acid; PBS, phosphate buffered saline; N/P ratios, nitrogen/phosphorus ratio, lipo2000, lipofectamine 2000; PCR, Polymerase Chain Reaction; SDS-PAGE, polyacrylamide gelelectrophoresis; PVDF, polyvinylidene difluoride; RPMI, roswell park memorial institute medium; TBS, tris-buffered saline; UV, Ultraviolet.

## 1 Introduction

Prostate cancer (PCa) has become one of the most commonly diagnosed malignancies in western countries and the second pathogenic factor of cancer-related deaths for men. In 2008, patients newly diagnosed with prostate cancer amounted to 14% of all tumor patients globally. While life quality and medical technology have improved, the occurrence of advanced prostate cancer has shown a rising trend. Patients with advanced prostate cancer usually had no indication to undergo a radical prostatectomy operation, and other traditional treatments such as chemotherapy are unable to effectively cure it. Therefore, seeking for new medication therapy for PCa is still a compelling challenge.

The emerging technique RNA interference (RNAi), based on small interfering RNAs (siRNAs) or microRNAs (miRNAs), has shown great potential in cancer treatment. In particular, RNAi possesses high specificity and the ability to regulate the expression of oncogenes in tumor initiation, growth and metastasis [1]. First discovered by Lee in 1993, miRNAs were non-coding small single stranded 18-24 nucleotides RNAs, participating in many significant biological processes including proliferation, cell differentiation, and apoptosis, and so on [2-3]. Recently, many studies have shown that miRNAs are associated

\*Corresponding author: Zhou JH, Xun L, Longgang District People's Hospital of Shenzhen, Guangdong 518000, China, E-mail: gdjh.zhou@163.com; gdgzlx@163.com

Chen CY, Li GY, Huang XH, Wu SC, Xu CZ: Longgang District People's Hospital of Shenzhen, Guangdong 518000, China

Zhang L, Cheng D: School of Chemistry and Chemical Engineering, Sun Yat-sen University, Guangzhou 510275, China

with various human diseases [4-7]. Aberrant expression of endogenous miRNAs has often been observed in human cancer tissues/cells and is believed to promote carcinogenesis and progression [8-12]. Furthermore, miRNA signatures unique to PCa have been identified as well and several onco-related miRNAs and tumor-suppressive miRNAs have been successfully identified [8-11]. For example, Visone has detected that expression of microRNAs (miR)-221/222 in prostate cancer tissues was significantly decreased, suggesting that miR-221/222 plays a critical role in the occurrence and growth of prostate cancer [13]. They found that supplement of exogenous miR-221/222 may regulate abnormal gene expression, thus inhibiting tumor growth. Besides, studies have shown that these two miRNAs play a significant role in tumorigenesis and progression, from androgen-dependent PCa to androgen-independent PCa [14-22].

Since the naked nucleic acids are unable to cross cell membranes and are susceptible to enzymatic degradation *in vivo*, the use of viral or non-viral carriers is crucial to overcome the poor intracellular uptake and restricted bloodstream stability [23]. Despite the high transfection efficiency in various cell types, the clinical applications of viral vectors are limited by immunogenicity, difficult preparation, and potential pathogenicity [24]. In comparison, non-viral vectors have presented as promising alternatives due to simple fabrication, lack of pathogenicity and immunogenicity, and better biocompatibility [25]. Non-viral vectors are synthesized through chemical processes that are basically divided into cationic polymers and cationic lipids because of its structure [26]. Among various non-viral vectors, polyethyleneimine (PEI) offers primary, secondary, and tertiary amines to construct with nucleic acids like DNA and miRNA. PEI is also a commonly studied cationic polymer in gene therapy. The PEI vector has many advantages, including high nucleic acid complexation efficiency, unique buffering effect for lysosomal escape, and easy modification with a targeting ligand to enable cell-type-specific interaction. However, PEI can induce cationic cytotoxicity, based on its concentration and molecular weight, because of its electrostatic interaction with negatively charged components in cell membrane, for instance, the sialic acid. Consequently, polyethylene glycol (PEG) as a non-charged hydrophilic polymer is usually bound to PEI to form PEG-g-PEI in order to eliminate cytotoxicity while keeping considerable delivery efficiency [27-31].

In an effort to search for an effective treatment of advanced prostate cancer, the present study aimed to show whether PEG-g-PEI is a promising nanocarrier with

good miRNA delivery efficiency and low cytotoxicity. The co-polymer PEG-PEI comprising PEG 2 kDa and PEI 25 kDa to mediate the delivery of miR-221/222 into PC-3 prostate cancer cells *in vitro*. The expression of tumor-suppressing SIRT1 gene regulated by the miRNA nanomedicine was evaluated.

## 2 Experimental procedures

### 2.1 Materials

The PC-3 prostate cancer cell line was produced by the type Culture Collection of the Chinese Academy of Sciences, Shanghai, China. Cell culture reagents were produced by GIBCO (Carlsbad, CA, USA). PEG-PEI was produced in our own lab as previously reported [32]. The miR-221/222, negative control miRNA and Cy3-labeled miRNAs were produced by RiboBio (Guangzhou RiboBio Co., Ltd.). Cell Counting Kit (CCK-8/WST-8) and AnnexinV-FITC Apoptosis Detection Kit were produced by KeyGen (KeyGen BioTECH, Guangzhou). The Taqman(r) microRNA RT Kit, TAQMAN UNIVERSAL MMIX II NO UNG and lipo2000 was produced by Life Technologies (Carlsbad, USA).

### 2.2 Cell culture

PC-3 prostate cancer cells were cultured in 1640 medium with 10% fetal bovine serum (FBS) under humidified conditions (37°C, 5% CO<sub>2</sub>). The cells were passaged on the third day, and were trypsinized and subcultured until they reached 90% confluence.

### 2.3 Synthesis of PEG-PEI

The PEG-PEI copolymer was produced and activated according to prior described method with minor modification [32]. PEG-OH was transformed to PEG-COOH through reacting with succinic anhydride (SA). After being dissolved in 20 mL anhydrous chloroform, PEG-OH and SA (1:5 in molar ratio) were refluxed at 70°C for 48 hours. When used distillation to eliminate chloroform polymer was dissolved again in 20 mL DI water and dialyzed against water for 2 days in order to remove succinic anhydride and residual succinic acid. It was then frozen to dry the product yielding purified PEG-COOH. Ultimately, hyperbranched PEI 25 kDa and NHS-activated PEG were

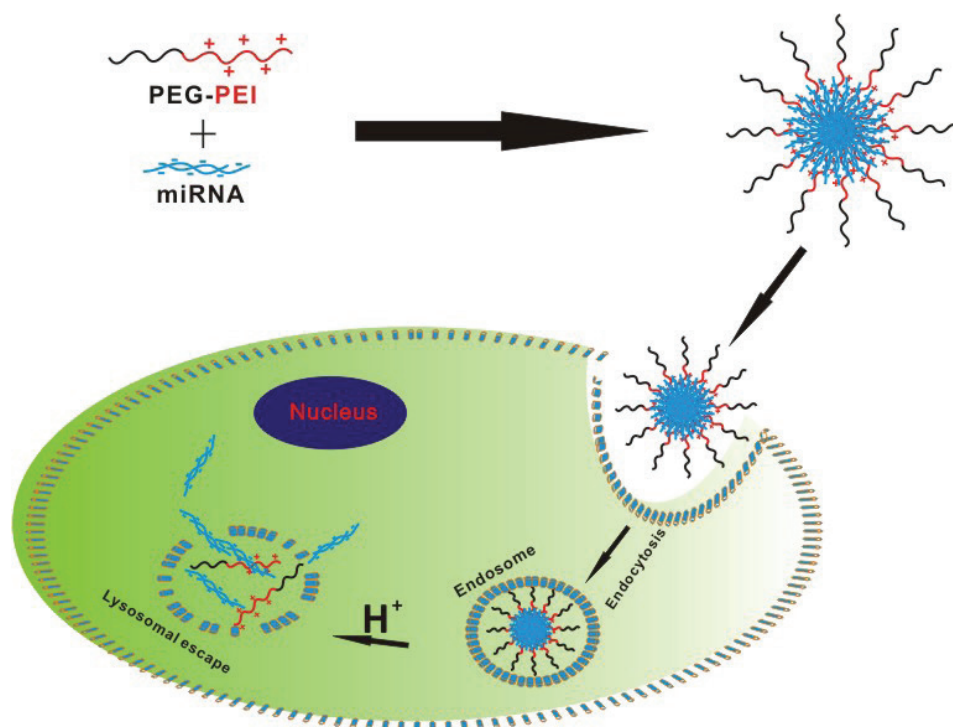


**Figure 1:** Schematic illustration of nanoparticle formation and internalization into PCa cells for co-delivery of miRNA.

reacted with DMSO and magnetically stirred during 24 hours at room temperature to form PEG-PEI. The solution was purified by membrane dialysis (MWCO: 14000 Da) in DI water during 3 days and the mixture was lyophilized Figure 1 .

## 2.4 Preparation of PEG-PEI/miR-221/222 nanoparticles

PEG-PEI was dissolved in RNase-free water with 1 mg/mL miR-221/222 was dissolved in water at 20 mM. Based on the designed N/P ratios, appropriate volumes of PEG-PEI and miR-221/222 mixture were combined, stirred for 15s, and incubated under room temperature for 30 min before use.

## 2.5 Gel retardation assay

Gel electrophoresis was used to determine the complexation of PEG-PEI with miRNA. According to the designed N/P ratios (0, 1, 2, 3, 4, 5), miR-221/222 (20 mM) was dissolved in 10x loading buffer before being transferred into 1% agarose gels with 0.5 mg/mL ethidium bromide (EB). The electrophoresis was conducted for 15 min at 130V. The miR-221/222 bands were visualized under UV light (Uvidoc, Cambridge, UK).

## 2.6 Measurement of particle size and zeta potential

2 mL of miR-221/222 was dissolved in DEPC water, mixed with PEG-PEI at different N/P ratios, and cultured at room temperature for 30 minutes. Afterwards, the mixed solution was diluted to 60 mL with DEPC-treated water. The potential and size were detected with the Zeta-Plus instrument (Brookhaven, New York) with detection angles of scattered light at 90° and 15°, respectively. Measurements were performed at room temperature. Result are shown in mean±SD (n=5).

## 2.7 Cell viability assay

CCK-8x assay was employed to test PC-3 cell viabilities at various cell incubation environments. PC-3 cells with density of  $5 \times 10^3$  cells per well were seeded onto the 96-well plates by 100 mL of 1640 medium with 10% FBS. The cells were cultured for 24 hours at 37°C and divided into 4 groups: blank control group, PEG-PEI/miR-221 group, PEG-PEI/miR-222 group and lipo2000 group. The medium was substituted with 100 mL fresh medium for every group prior to the experiment. Based on the N/P ratios of 0, 1, 2, 5, 10, 20, 50, 100, 200, different amounts of PEG-PEI/miRNA mixture were placed into the medium, and then

the incubated plates were slightly wobbled and placed for 48 hours. After that, 10 mL of CCK-8 solution was mixed into each well to continue incubate for 2 hours under the dark conditions. The Infinite F200x Multimode Plate Reader (Tecan, Crailsheim, Germany) was used to obtain light absorption data for each well at 450 nm wavelength. The experiments were then repeated twice so that all groups have three replicates. The dose in each well of the miR-221/222 and miR-scr was 100 nM.

## 2.8 *In vitro* transfection

The flow cytometry was used to detect the transfection efficiency of nanoparticles *in vitro* at different N/P ratios. PC-3 cells were placed onto a 6-well plate with density of  $5 \times 10^4$  cells in each well then incubated for 24 hours. 6 mL of Cy3-labeled miR-scr was complexed with polymer or lipo2000 at different N/P ratios (2, 4, 10, 20) by gently mixing for 30 min. The blank group received normal cell culture in the absence of nanoparticles, and the other groups were incubated with PEG-PEI/miR-scr or lipo2000/miR-scr. The dose per well of Cy3-labeled miR-scr was 100 nM. Cells were then rinsed twice with PBS, and the nanomedicine solution was added to each well to reach a volume of 100 mL in 1640 medium. After 8 h incubation, each well was rinsed 3 times with PBS and mixed with 0.25% trypsin/EDTA to suspend the cells. The cells were finally converted into tubes for determining transfection efficiency with flow cytometry (Gallios, Beckman Coulter, USA).

## 2.9 Laser confocal microscopy assay

The transfection efficiency of nanoparticles prepared at 20 N/P ratio was evaluated in PC-3 cells with laser confocal microscope. PC-3 cells were seeded onto a petri dish at density of  $3 \times 10^3$  cells each well and normally cultured for 24 h. Then, the PEG-PEI/miR-scr (miR-scr was labeled with Cy3) to incubate the cells for 6 h. Afterwards, the cells were rinsed 3 times with PBS, and Hoechst and LysoTracker Green were added to stain the nuclei and lysosomes according to the manufacturer's protocols. The PBS rinsed cells were visualized by the Zeiss LSM 710 confocal microscope (Carl Zeiss Co., Ltd., Gottingen, Germany).

## 2.10 RT-PCR

PC-3 cells were seeded onto 6-well plates and incubated for 24 hours. We artificially divided the cells for 4

groups: PEG-PEI/miR-221/222 group (N/P=20), PEG-PEI/miRNA-scr group (N/P=20), lipo2000/miR-221/222 group, and the control group. Again, experiments were repeated so that all groups have three replicates. Total RNA was extracted with Trizol reagent (Invitrogen, Carlsbad, CA, USA) after the cells were transfected for 24 hours. Real-time PCR was performed as described in PrimeScript PCR Kit instructions. Assays with sequences of miR-221/222 were listed as follows: hsa-miR-221-3p: AGCUACAUGUCUGCGGGUUUC, hsa-miR-222-3p: AGCUACAUCUGGCUACUGGGU. Control miRNA sequences (U6 snRNA): 5'-GGAACGATACAGAGAAGATTAGCA-3' [33]. The programs were placed under the thermal cycling environment of 95 °C/10 min, followed by 40 cycles of 95 °C/15 s, 60 °C/60 s.

## 2.11 Western blotting assay

PC-3 cells seeded onto 6-well plates were divided into 4 groups: PEG-PEI/miR-221/222 group (N/P=20), PEG-PEI/miRNA-scr group (N/P=20), lipo2000/miR-221/222 group, and the control group. Cells were harvested after 48 hours of transfection. We then collected the total protein in order to detect the concentration through bicinchoninic acid protein assay kit (Sheng Gong Bio-Tech Co, Ltd, Shanghai, China). SDS-PAGE was used to separate different protein samples, which were then transferred onto polyvinylidene difluoride (PVDF) membranes. After being blocked with 5% skim milk for 2 hours, the membranes were incubated overnight with primary antibody (1:2000 dilution, CST, USA) at 4 °C, and placed with the secondary anti-rabbit IgG-horseradish peroxidase (1:2000 dilution, CST, USA) for 1 hour at room temperature. The blots were cultured with enhanced chemiluminescence for 2 min. These protein bands were visualized under UV light. Overall, the  $\beta$ -actin was used as an endogenous control to normalize the data for protein expression.

## 2.12 Statistical analysis

All tests were required to repeat at least 3 times, and statistical analyses of the data were displayed with SPSS 17.0 software. Final results are shown as the mean  $\pm$  standard deviation (SD), and statistical significance (SF) was obtained at  $P < 0.05$ .

Ethical approval: The conducted research is not related to either human or animal use.



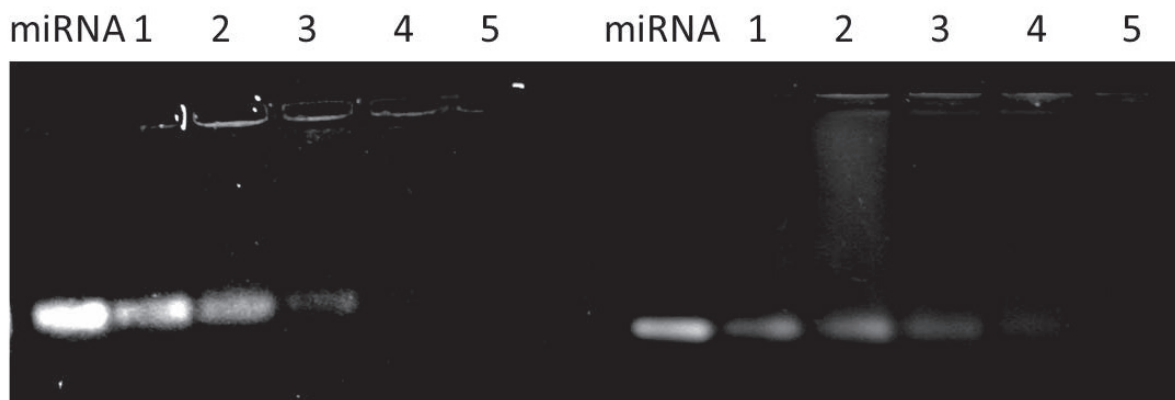


**Figure 2:** Electrophoresis of PEG-PEI/miR-221 (a) and PEG-PEI/miR-222 (b) formed at various N/P ratios and miR-221/222 dose of 100 nM.

### 3 Results

#### 3.1 Gel retardation assay

PEG-PEI/miR-221/222 nanoparticles with various N/P ratios were subjected to the agarose gel electrophoresis. It is well-known that when the negative charge of miRNAs is neutralized by the positive charge of cationic polymers, its motion in the gel will be retarded. In addition, RNA complexed with polymer is unable to gain an insertion of the ethidium bromide (EB). The intensity of miRNA bands reduced when N/P ratios increased from 0 to 5 (Figure 2). At the N/P ratio of 4, the miRNAs band totally disappeared, meaning that the miRNAs were fully complexed by PEG-PEI.

#### 3.2 Size and zeta potential of PEG-PEI/miR-221/222 polyplexes

Following with the increasing of N/P ratio of PEG-PEI/miR-221/222, the size decreased whereas the zeta potential raised (Figure 3). At N/P ratio of 4, the PEG-PEI/miR-221 polyplex measured  $171 \pm 9$  nm and  $6.12 \pm 0.31$  mV in size and zeta potential, respectively. In contrast, at N/P ratio of 20, the size of the polyplex decreased to  $116 \pm 6$  nm whereas the zeta potential increased to  $21.34 \pm 1.07$  mV. The data of PEG-PEI/miR-222 polyplex were similar to that of PEG-PEI/miR-221.

#### 3.3 Cytotoxicity of PEG-PEI

The CCK-8 assay could detect the cytotoxicity of PEG-PEI and PEG-PEI/miR-scr nanoparticles 24 h after transfection

(Figure 4). Generally, the cytotoxicity of PEG-PEI was also elevated when the concentration of polymer increased. At the PEG-PEI concentration of 50 mg/mL, the cell viability was  $78.30 \pm 3.92\%$ . Over this concentration value, the cell viability was conspicuously reduced following with increase in polymer concentration. Considering the PEG-PEI/miR-scr polyplex, cytotoxicity was clearly shown at very high value of N/P ratio that over 20. Below this threshold value, the cells still kept the high viability over 90%. It referred to complexation with siRNA reduced the positive charge presented in polymeric vector, that triggered the cationic cytotoxicity decreased. Over an N/P ratio of 20, large amount of excessive cationic PEG-PEI was present in the solution, which would limit cell development. For instance, when the N/P ratio was up to 100, the cell viability of PEG-PEI/miR-scr was decreased  $68.85 \pm 3.44\%$ .

#### 3.4 In vitro transfection efficiency

The transfection efficiency of the polyplexes of PEG-PEI and Cy3-labeled miR-scr in PC-3 cells was determined using flow cytometry. The transfection efficiencies varied at different N/P ratios (Figure 5). While the N/P ratio raised to 20 from 2, the transfection efficiencies increased to  $99.75 \pm 4.99\%$  from  $1.15 \pm 0.06\%$ , which reached the level for the positive control lipo2000 ( $99.65 \pm 4.99\%$ ).

#### 3.5 Cell uptake

Cell uptake of PEG-PEI/Cy3-labeled miR-scr polyplexes (N/P=20) was detected using confocal laser scanning microscopy (CLSM). Red fluorescence was distributed in the synapses of PC-3 prostate cancer cells and cytoplasm

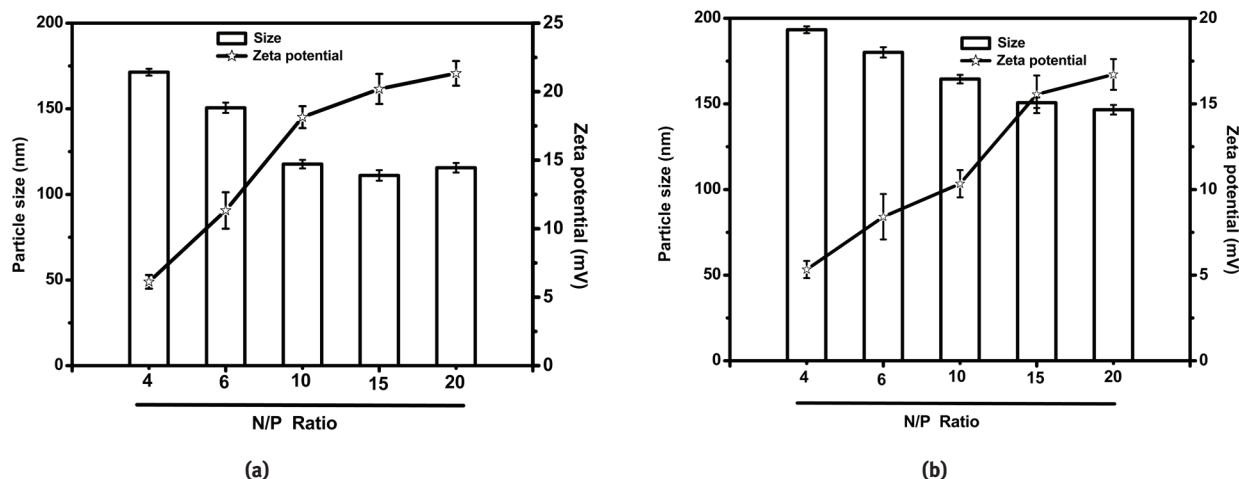


**Figure 3:** The particle sizes, zeta-potentials of PEG-PEI/miR-221 (a) and PEG-PEI/miR-222 (b) polyplexes formed at different N/P ratios. Measurements were performed at room temperature, and data shown in mean $\pm$ SD (n=5).

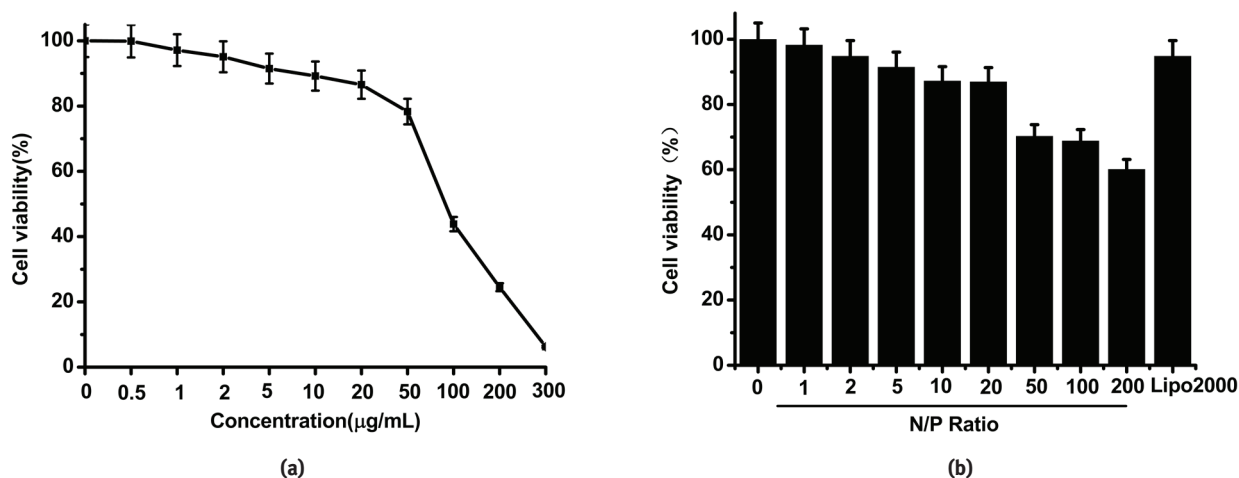


**Figure 4:** (a) Left: Cytotoxicity of PEG-PEI in PC-3 cells determined by a CCK-8 assay. PC-3 cells were treated with PEG-PEI at various concentrations from 0 to 300  $\mu$ g/mL. (b) Right: Cytotoxicity of PEG-PEI/miR-scr polyplexes in PC-3 cells at various N/P ratios from 0 to 200. The dose of miR-scr was 100 nM per well and incubation time was 24 hours.

(Figure 6). Furthermore, the lysosomes were stained green by LysoTracker green and labeled nuclei by blue with Hoechst. By merging the three fluorescent images, it was clear that the red fluorescence partially co-localized with the green fluorescence in the lysosomes.

### 3.6 The cytotoxicity of PEG-PEI/miR221/222 determined by CCK-8 assay

CCK-8 assay was used to evaluate the cytotoxicity of PEG-PEI/miR-221/222 polyplexes (N/P=20) 24 hours after transfection (Figure 7). PEG-PEI/miR-scr polyplex was nearly non-cytotoxic. The PC-3 cells incubated with it remained high viability during range of 95.49 $\pm$ 4.77%.

In comparison, PEG-PEI/miR-221 and PEG-PEI/miR-222 showed clear cytotoxicities by revealing significantly reduced cell viabilities down to the ranges of 67.83 $\pm$ 3.39% and 61.49 $\pm$ 3.07%, respectively. This suppression of PC-3 cells development was clearly due to the target gene regulation effect of miR-221 and miR-222, as well be further confirmed in the next section.

### 3.7 SIRT1 expression

The cancer cells were transfected with PEG-PEI/miR-221/222 polyplexes and the target gene regulation was confirmed by RT-PCR and western blot assays. Compared to the LN and the PN groups, the miR-221/222 transfection

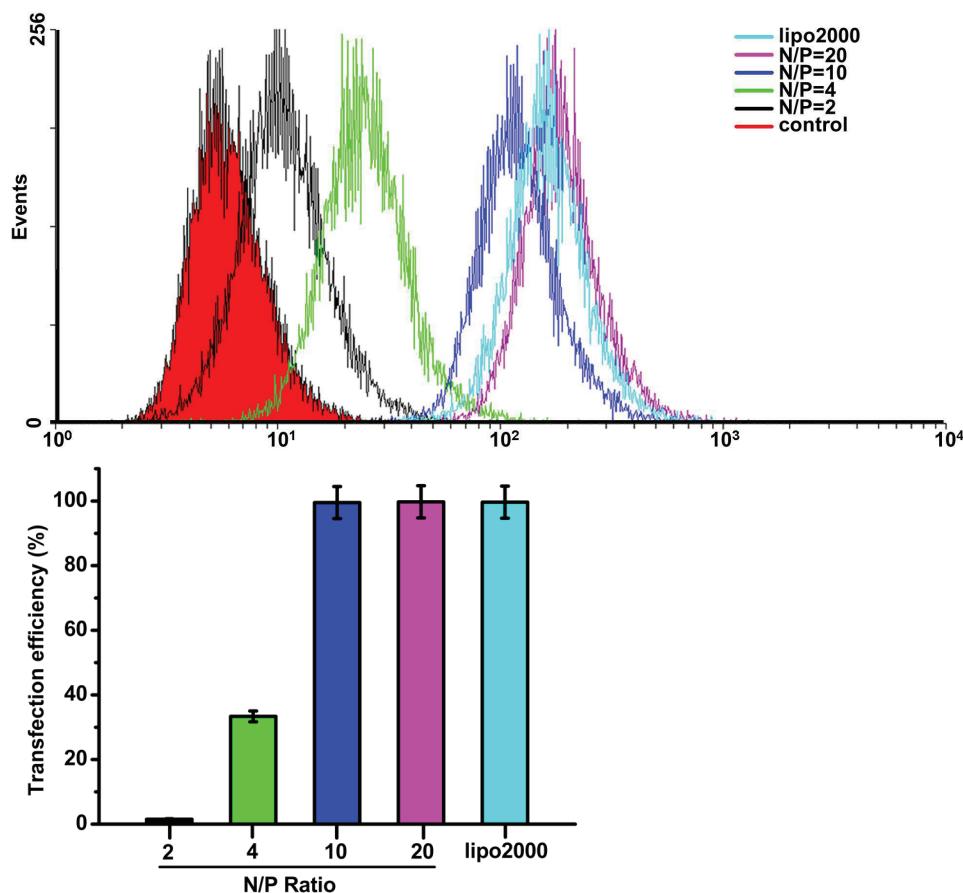


**Figure 5:** (a) The ratio of Cy3-positivexcells investigated by flow cytometry ( $n=3$ ). Incubation time: 6 h. Dose: 100 nM miRNAs. (b) The transfection efficiencies varied at different N/P ratios.

of PC-3 cells in the L1/L2 and P1/P2 trials resulted in higher SIRT1 expression with the mRNA level (Figure 8 a,b). Moreover, the polymeric vector appeared even more effective than the positive control lipo2000 in mediating the miR-221 and miR-222 transfection which upregulated the SIRT1 expression, i.e.  $70.85 \pm 3.54\%$  (P1) vs  $46.37 \pm 2.32\%$  (LI) and  $55.58 \pm 2.78\%$  (P2) vs  $44.2 \pm 2.21\%$  (L2). Western blot analysis gained consistent measurement at the protein level of SIRT1 expression. SIRT1 protein levels transfected with PEG-PEI/miR-221/222 were remarkably higher compared with that in cells transfected with lipo2000/miR-221/222 (Figure 8 c,d), which indicates that the miR-221/222 were successfully delivered into PC-3 cells by PEG-PEI and effectively released inside cells.

## 4 Discussion

As the result of miR-221, miRanda data, and miR-222 are connected to the specific sequences located at the 3'-

UTR of SIRT1 mRNA. In addition, among the 16 genes involved in cancer, five are specifically related to prostate cancer (BTG2, IGFBP3, SIRT1, MXI1, and FDPS) [34]. In PCa, SIRT1 has been engaged in autophagy, and SIRT1 knockdown triggered PIN growth, referring to SIRT1 might act as a tumor suppressor gene in the cancer model [35]. Furthermore, Yang and Gan have confirmed that miR-221 and miR-222 did not connect to the SIRT1xsequence immediately via the luciferase activity assay [36], which illustrates that miR-221 and miR-222 indirectly enhanced the expression of SIRT1 from other molecular pathways, such as p27 [37] or ARH [38].

In the present research, we tried to deliver miR-221 and miR-222 to PC-3 prostate cancer cells through a polymeric vector PEG-PEI in order to overexpress the two miRNAs and thus modulate the expression of SIRT1, which is involved in the PCa pathogenesis. Upon polyplex formation, the agarose gel electrophoresis showed that the miR-221/222 bands disappeared at the N/P ratios above 4, indicating complete complexation of miR-221/222

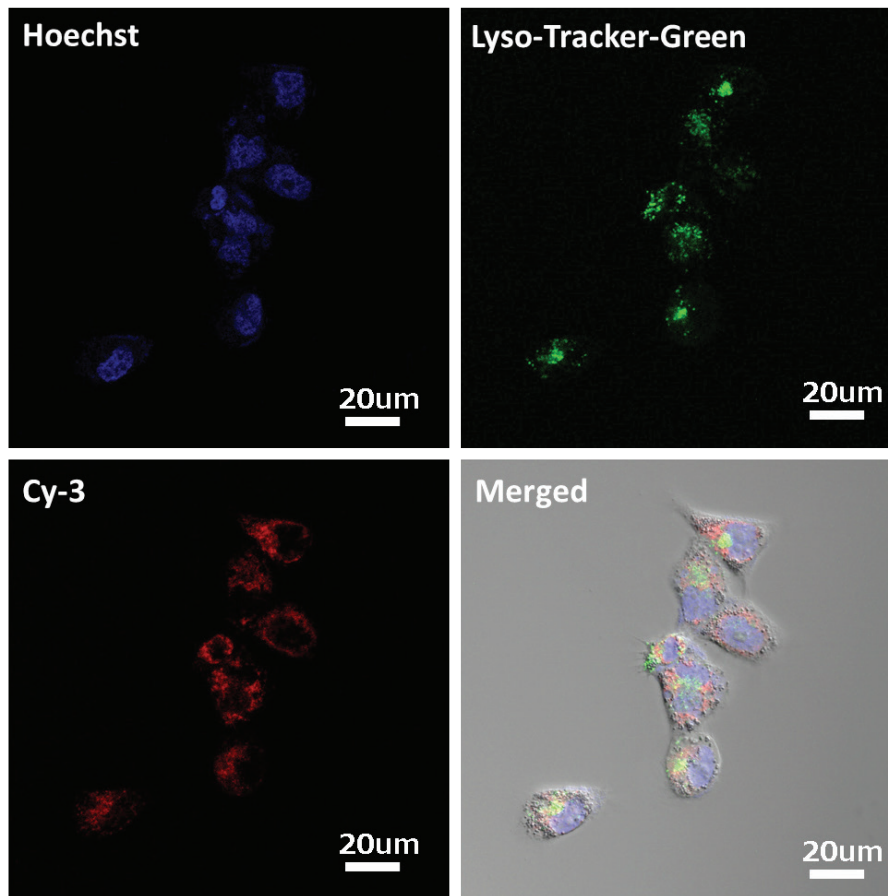


**Figure 6:** High magnification ( $\times 400$ ) laser confocal microscopic images of PC-3 cells incubated with PEG-PEI/miR-scr polyplexes ( $N/P=20$ ). Dose of miR-scr: 100nM. Blue: nuclei stained with Hoechst; red: miR-scr labeled with Cy3; green: lysosomes labeled with Lyso-Tracker green.

- a: Figure of nuclei stained with Hoechst  
 b: Figure of lysosomes labeled with Lyso-Tracker green  
 c: Figure of miR-scr labeled with Cy3  
 d: Figure of merging the three fluorescent images

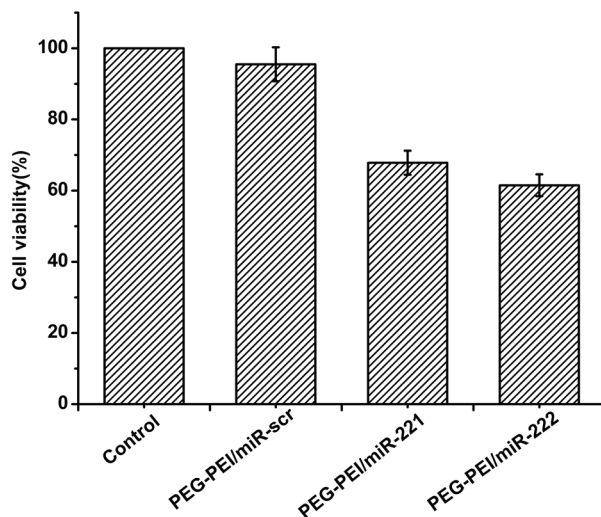


**Figure 7:** Viabilities of PC-3 cells treated with different samples. Three polyplexes were all synthesized at  $N/P=20$ .

in these polyplexes. The particle size and zeta potential of the polyplexes affected the stability of the polyplexes in bloodstream [39], and should be controlled in order for miRNAs to cross the cell membrane more easily. Consequently, the particle size and zeta potential are crucial for the cellular uptake *in vitro* and transfection efficiency of polyplexes. Our data indicated that the particle size of polyplexes was reduced to  $116 \pm 6$  nm from  $171 \pm 9$  nm while the ratio was raised to  $N/P=20$  from  $N/P=4$ , according to the interaction of PEG-PEI and miR-221/222 resulting in the compaction of polyplexes at high  $N/P$  ratios. The excess positive charge of PEG-PEI led to high zeta potential. The zeta potential of polyplexes increased to  $21.34 \pm 1.07$  mV from  $6.12 \pm 0.31$  mV when the  $N/P$  ratio raised to  $N/P=20$  from  $N/P=4$ . It is difficult to select a suitable  $N/P$  ratio for small particle size and meanwhile low zeta potential. Thus, a cytotoxicity test was conducted for



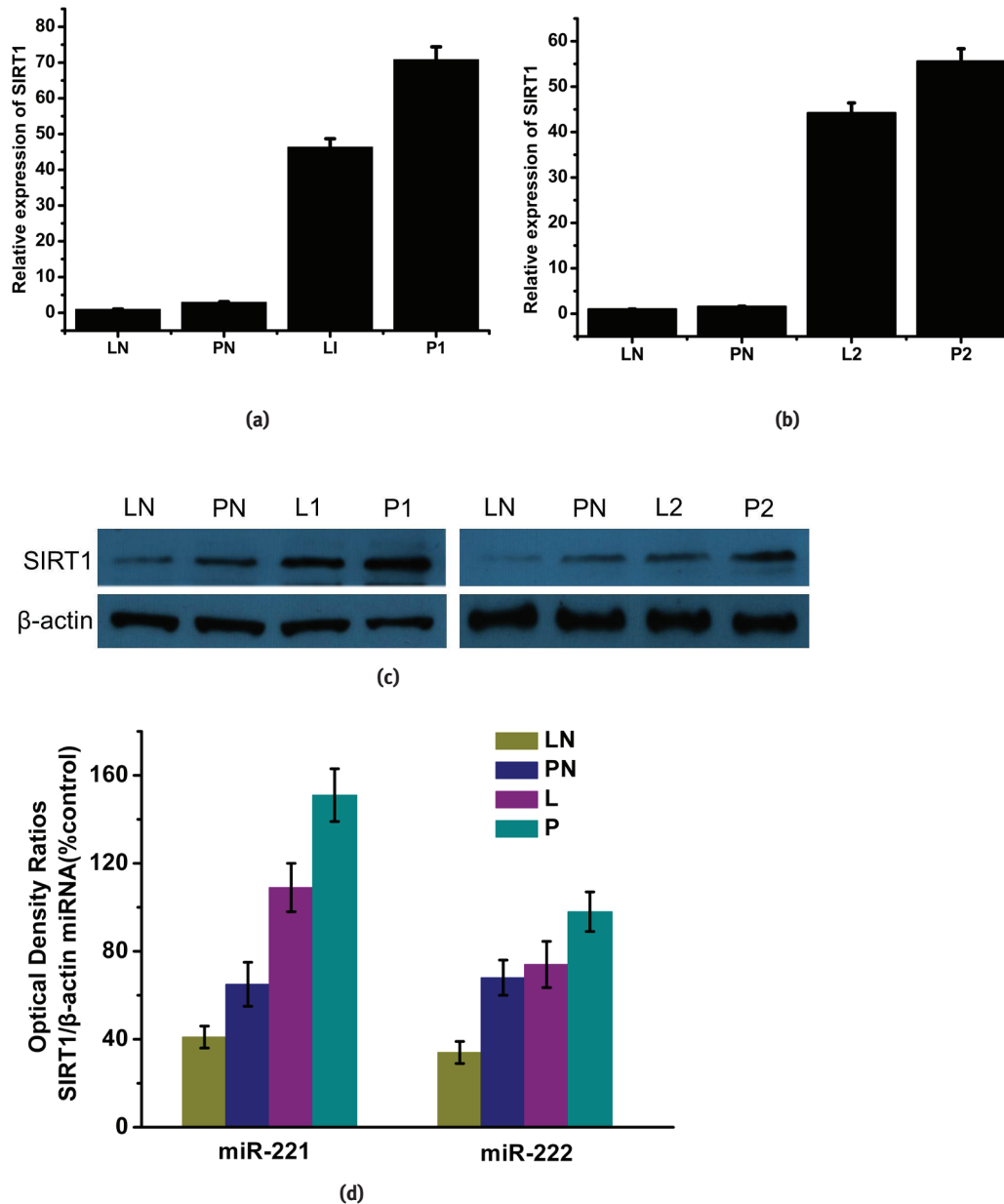


**Figure 8:** (a) Figure of SIRT1 gene expression in PC-3 cells by RT-PCR.(miR-221 group). (b) Figure of SIRT1 gene expression in PC-3 cells by RT-PCR.(miR-222 group) LN: blank group; PN: PEG-PEI/miR-scr group; L1: lipo2000/miR-221 group; P1: PEG-PEI/miR-221 group; L2: lipo2000/miR-222 group; P2: PEG-PEI/miR-222 group. Dose of miR: 100nM; polyplexes were synthesized at N/P=20; data are mean $\pm$ SD (n=3). (c) Analysis of SIRT1 expression at protein level by western blot. (d) The densitometric data of western blot LN: blank group; PN: PEG-PEI/miR-scr group; L:lipo2000/miR-221 group (lipo2000/miR-222 group); P: PEG-PEI/miR-221 group (PEG-PEI/miR-222 group). Dose of miR: 100nM; polyplexes were formed at N/P=20.

PEG-PEI/miR-221/222 polyplexes with different N/P ratios. CCK-8 assay was conducted to analyze the cytotoxicities of PEG-PEI, PEG-PEI/miR-scr and PEG-PEI/miR-221/222 polyplexes with different N/P ratios. Complexation with miR decreased the cytotoxicity of PEG-PEI. Our results showed that the cytotoxicity of the PEG-PEI/miR-scr polyplex in PC-3 cells increased along with the increase of N/P ratio. When the N/P ratio reached above 100, the cell

viability decreased to below 70%, which was much lower than that caused by lipo2000/miR-scr (94.85 $\pm$ 4.74%) and thus considered not suitable for biological studies. In comparison, the cells remained high viability above 90% at N/P ratios below 20.

Based on the results, biological experiments were performed using the PEG-PEI/miR-scr polyplex formed at N/P=20. At this N/P ratio, the transfection efficiency

of PEG-PEI/miR-221/222 polyplexes (N/P=20) in PC-3 cells reached  $99.75 \pm 4.99\%$  which was equivalent to lipo2000/miR-scr ( $99.65 \pm 4.99\%$ ), according to flow cytometric analysis. The cell uptake of Cy3-labeled PEG-PEI/miR-scr was also investigated with confocal laser scanning microscopy. Nanoparticles react with the cell membrane through endocytosis process, which triggers the uptake of the nanoparticles [40]. Our data proved that the PEG-PEI/miR-scr was able to across the cell membrane. Moreover, the red fluorescence from Cy3-labeled miR-scr only partially overlapped with the green fluorescence of lysosomes, which indicate that free miR-scr was released and distributed outside the lysosome from polyplex. Consequently, transfection of PC-3 cells with PEG-PEI/miR-221 and PEG-PEI/miR-222 polyplexes resulted in  $67.83 \pm 3.39\%$  and  $61.49 \pm 3.07\%$  viabilities, indicating the effective suppression of cell developing using PEG-PEI/miR-221/222.

To further verify the potential for future in vivo application, The PC-3 prostate cancer cells were transfected with PEG-PEI/miR-221/222 polyplexes and the target gene regulation was confirmed by RT-PCR and western blot assays. Our results showed that at N/P=20 the PEG-PEI/miR-221/222 polyplexes more effectively promoted the gene expression of SIRT1 than the positive control (lipo2000//miR-221/222).

## 5 Conclusion

In conclusion, we successfully fabricated PEG-PEI/miR-221/222 polyplexes to modulate the SIRT1 gene in PC-3 prostate cancer cells *in vitro*. The polyplexes exhibited a low cytotoxicity and high transfection efficiency. Although several medical therapies, e.g. radical prostatectomy or radiation therapy, are present for localized disease, about one third of healing patients will relapse. In many cases, cancer progresses despite initial treatment progress with androgen ablation therapy turning into the hormone-refractory prostate cancer (HRPC) which is highly resistant to conventional chemotherapies [41]. Therefore, the PEG-PEI/miR-221/222 polyplexes may be a new medication option for prostate cancer especially for the HRPC. Our data indicate that PEG-PEI/miR-221/222 could effectively promoted SIRT1 expression, giving the basis for future in vivo study to treat HRPC.

**Acknowledgements:** We thank the colleagues in our lab of the School of Chemistry and Chemical Engineering, Sun Yat-sen University; Li CX, Xiao H, Chen JB and Fang JT for helping synthesized the PEG-PEI.

**Conflict of interest:** Authors declare no conflict of interest.

## References

- [1] Vaishnav A.K., Gollob J., Gamba-Vitalo C., Hutabarat R., et al., A status report on RNAi therapeutics, *Silence.*, 2010, 1(1), 1-13.
- [2] Lee R.C., Feinbaum R.L., Ambros V., et al., The C elegans heterochronic gene lin-4 encodes small RNAs with antisense complementarity to lin-4, *Cell.*, 1993, 75(7), 843-854.
- [3] Ambros V., et al., The functions of animal microRNAs, *Nature.*, 2006, 431, 350-355.
- [4] Esquela-Kerscher A., Slack F.J., et al., Oncomirs-microRNAs with a role in cancer, *Nat Rev Cancer.*, 2006, 6, 259-269.
- [5] Iorio M.V., Ferracin M., Liu C., Veronesi A., Spizzo R., et al., MicroRNA gene expression deregulation in human breast cancer, *Cancer Res.*, 2005, 65, 7065-7070.
- [6] Latronico M.V., Catalucci D., Condorelli G., et al., Emerging role of microRNAs in cardiovascular biology, *Circ Res.*, 2007, 101, 1225-1236.
- [7] Lynam-Lennon N., Maher S.G., Reynolds J.V., et al., The roles of microRNA in cancer and apoptosis, *Biol Rev Camb Philos Soc.*, 2009, 84, 55-71.
- [8] Ozen M., Creighton C.J., Ozdemir M., Ittmann M., et al., Widespread deregulation of microRNA expression in human prostate cancer, *Oncogene.*, 2008, 27, 1788-1793.
- [9] Porkka K.P., Pfeiffer M.J., Waltering K.K., Vessella R.L., et al., MicroRNA expression profiling in prostate cancer, *Cancer Res.*, 2007, 67, 6130-6135.
- [10] Schaefer A., Jung M., Mollenkopf H.J., et al., Diagnostic and prognostic implications of microRNA profiling in prostate carcinoma, *International Journal of Cancer.*, 2009, 126(5), 1166-1176.
- [11] Volinia S., Calin G.A., Liu C.G., Ambs S., et al., A microRNA expression signature of human solid tumors defines cancer gene targets, *Proc Natl Acad Sci U S A.*, 2006, 103, 2257-2261.
- [12] Lu J., Getz G., Miska E.A., Alvarez-Saavedra E., et al., MicroRNA expression profiles classify human cancers, *Nature.*, 2005, 435, 834-838.
- [13] Visone R., Pallante P., Vecchione A., et al., Specific microRNAs are downregulated in human thyroid anaplastic carcinomas, *Oncogene.*, 2007, 26(54), 7590-7595.
- [14] Chen W.X., Hu Q., Qiu M.T., Zhong S.L., Xu J.J., et al., miR-221/222: promising biomarkers for breast cancer, *Tumour Biol.*, 2013, 34, 1361-1370.
- [15] Chun-Zhi Z., Lei H., An-Ling Z., Yan-Chao F., Xiao Y., et al., MicroRNA-221 and microRNA-222 regulate gastric carcinoma cell proliferation and radioresistance by targeting PTEN, *BMC Cancer.*, 2010, 10, 367.
- [16] Garofalo M., Di Leva G., Romano G., Nuovo G., Suh S.S., et al., miR-221&222 regulate TRAIL resistance and enhance tumorigenicity through PTEN and TIMP3 downregulation, *Cancer Cell.*, 2009, 16, 498-509.
- [17] Hao J., Zhang C., Zhang A., Wang K., Jia Z., et al., miR-221/222 is the regulator of Cx43 expression in human glioblastoma cells, *Oncology Reports.*, 2012, 27(5), 1504-1510.

- [18] Jikuzono T., Kawamoto M., Yoshitake H., Kikuchi K., Akasu H., et al. The miR-221/222 cluster, miR-10b and miR-92a are highly upregulated in metastatic minimally invasive follicular thyroid carcinoma, *J. International Journal of Oncology*, 2013, 42(6), 1858–1868.
- [19] Shah MY., Calin GA., et al., MicroRNAs miR-221 and miR-222: a new level of regulation in aggressive breast cancer, *Genome Med.*, 2011, 3, 56.
- [20] Sun T., Yang M., et al., Role of microRNA-221/-222 in cancer development and progression, *Cell Cycle*, 2009, 8, 2315–2316.
- [21] Mercatelli N., Coppola V., Bonci D., et al., The inhibition of the highly expressed miR-221 and miR-222 impairs the growth of prostate carcinoma xenografts in mice, *PLoS One*, 2008, 3, e4029.
- [22] Sun T., Wang Q., Balk S., Brown M., Lee G.S., et al., The role of microRNA-221 and microRNA-222 in androgen-independent prostate cancer cell lines, *Cancer Res.*, 2009, 69, 3356–3363.
- [23] Costa P.M., Pedrosa de Lima M.C., et al., MicroRNAs as Molecular Targets for Cancer Therapy: On the Modulation of MicroRNA Expression, *Pharmaceuticals*, 2013, 6(10), 1195–1220.
- [24] Kim W.J., Kim S.W., et al., Efficient siRNA delivery with non-viral polymeric vehicles, *Pharm. Res.*, 2009, 26, 657–666.
- [25] Takahashi Y., Nishikawa M., Takakura Y., et al., Nonviral vectormediated RNA interference: its gene silencing characteristics and important factors to achieve RNAi-based gene therapy, *Adv. Drug Deliv. Rev.*, 2009, 61, 760–766.
- [26] Jing G.J., Fu Z.G., Dan B., et al., Development and evaluation of a novel nano-scale vector for siRNA, *Cell. Biochem.*, 2010, 111, 881–888.
- [27] Fischer D., Bieber T., Li Y., et al., A novel nonviral vector for DNA delivery based on low molecular weight, branched polyethylenimine: effect of molecular weight on transfection efficiency and cytotoxicity, *Pharm Res.*, 1999, 16(8), 1273–1279.
- [28] Ogris M., Brunner S., Schüller S., et al., PEGylated DNA/ transferrin-PEI complexes: reduced interaction with blood components, extended circulation in blood and potential for systemic gene delivery, *Gene Ther.*, 1999, 6(4), 595–605.
- [29] Fischer D., von Harpe A., Kunath K., et al., Copolymers of ethylene imine and N-(2-hydroxyethyl)-ethylene imine as tools to study effects of polymer structure on physicochemical and biological properties of DNA complexes, *Bioconjug Chem.*, 2002, 13(5), 1124–1133.
- [30] Fischer D., Osburg B., Petersen H., et al., Effect of poly(ethylene imine) molecular weight and pegylation on organ distribution and pharmacokinetics of polyplexes with oligodeoxynucleotides in mice, *Drug Metab Dispos.*, 2004, 32(9), 983–992.
- [31] Merkel O.M., Librizzi D., Pfestroff A., et al., Stability of siRNA polyplexes from poly(ethylenimine) and poly(ethylenimine)-g-poly(ethylene glycol) under in vivo conditions: effects on pharmacokinetics and biodistribution measured by fluorescence fluctuation spectroscopy and single photon emission computed tomography (SPECT) imaging, *J. Control Release*, 2009, 138(2), 148–159.
- [32] Chen G., Chen W., Wu Z., Shuai X., et al. MRI-visible polymeric vector bearing CD3 single chain antibody for gene delivery to T cells for immunosuppression, *Biomaterials*, 2009, 30, 1962–1970.
- [33] Turner M., Adhikari S., Subramanian S., et al. Optimizing stem-loop qPCR assays through multiplexed cDNA synthesis of U6 and miRNAs, *Plant Signal Behavior*, 2013, 8(8), e 24918.
- [34] Long Q., Xu J., Osunkoya A.O., et al., Global transcriptome analysis of formalin-fixed prostate cancer specimens identifies biomarkers of disease recurrence, *Cancer Res.*, 2014, 74(12), 3228–3237.
- [35] Powell M.J., Casimiro M.C., Cordon-Cardo C., et al., Disruption of a Sirt1-dependent autophagy checkpoint in the prostate results in prostatic intraepithelial neoplasia lesion formation, *Cancer research*, 2011, 71(3), 964–975.
- [36] Yang X., Yang Y., Gan R., et al., Down-regulation of mir-221 and mir-222 restrain prostate cancer cell proliferation and migration that is partly mediated by activation of SIRT1, *PLoS One*, 2014 Jun 3, 9(6), <https://doi.org/10.1371/journal.pone.0098833>
- [37] Galardi S., Mercatelli N., Giorda E., Massalini S., Frajese G.V., et al., miR-221 and miR-222 expression affects the proliferation potential of human prostate carcinoma cell lines by targeting p27Kip1, *J. Biol Chem.*, 2007, 282, 23716–23724.
- [38] Chen Y., Zaman MS., Deng G., Majid S., Saini S., et al., MicroRNAs 221/222 and Genistein-Mediated Regulation of ARHI Tumor Suppressor Gene in Prostate Cancer, *Cancer Prevention Research*, 2010, 4, 76–86.
- [39] Liang Y., Liu Z., Shuai X., Wang W., et al., Delivery of cationic polymer-siRNA nanoparticles for gene therapies in neural regeneration, *Biochem Biophys Res Commun.*, 2012, 421, 690–695.
- [40] Martins S., Costa-Lima S., Carneiro T., et al., Solid lipid nanoparticles as intracellular drug transporters: an investigation of the uptake mechanism and pathway, *Int. J. Pharm.*, 2012, 430, 216–227.
- [41] Shah R.B., Mehra R., Chinnaiyan A.M., et al., Androgen independent prostate cancer is a heterogeneous group of disease: lessons from a rapid autopsy program, *Cancer Research*, 2004, 64, 9029–9216.